

Green synthesis of magnesium oxide nanoparticles using *Gmelina arborea* leaf extract: antimicrobial, antioxidant, and antiangiogenic potentials

P. Shivappa¹, A. T. Gaddigal¹, P. B. Poojari¹, K. M. Irannanavar¹, P. V. Huyilagolaa¹, S. V. Irannanavar², C. M. Kamanavalli^{1*}

¹P.G. Department of Studies in Biochemistry, Karnatak University, Dharwad - 580 003, India. ²Sushruta Institute of Ayurvedic Medical Sciences and Research Center, Davanagere - 577 005, India.

Submitted on: 07-Apr-2025, Accepted and Published on: 12-May-2025

Article

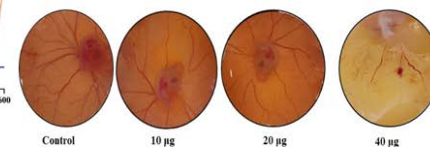
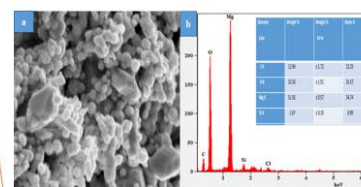
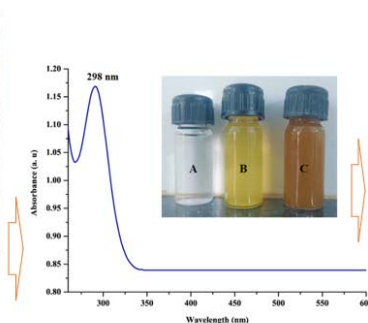
ABSTRACT

This study focuses on the green synthesis of magnesium oxide nanoparticles (MgO NPs) using the aqueous leaf extract of *Gmelina arborea* (*G. arborea*). The



Gambhari
Gmelina Arborea

+ MgO



NPs were characterized using various spectroscopic techniques. The UV-visible (UV-vis) absorption peak at 298 nm, Fourier transform infrared analysis confirms the chemical composition and molecule or ligand on the surface of NPs, and X-ray diffraction peaks show well crystalline nature of MgO NPs. The dynamic light scattering (DLS) analysis displayed an average particle size of 67 ± 10 nm, and the zeta potential (ZP) was found to be -36 ± 5 mV scanning electron microscopy (SEM) and high-resolution transmission electron microscopy (HR-TEM) analyses exhibit spherical morphology of NPs. The presence of C, O, and Mg elements confirmed by the energy-dispersive X-ray spectroscopy (EDX) analysis. Thermal behaviour of NPs exhibits multistage decomposition which is analysed by thermogravimetric (TG) analysis and exothermic process done by differential scanning calorimetry (DSC). The NPs showed notable antibacterial activity against human bacterial pathogens. The synthesized MgO NPs demonstrated strong antioxidant (> 75%) activity with IC_{50} value $96.8 \mu\text{g/mL}$ compared to leaf extract. Furthermore, MgO NPs shows anti-angiogenic properties in dose dependent manner. The study emphasizes the potential of *G. arborea* as a plant source for green synthesis and biomedical applications.

Keywords: MgO nanoparticles, Green chemistry, Physico-chemical properties, Antibacterial, Anti-angiogenic, DPPH assay

INTRODUCTION

The multidisciplinary field of nanoscience, which combines physics, chemistry, biology, and material science, has grown rapidly in recent decades, resulting in advancements in energy, agriculture, medicine, and nanoelectronics [1, 2]. Green chemistry strategy is essential for extensive use in nanotechnology and biological integration is preferred over chemical and physical processes for producing nanoparticles due to its ease, robust, affordability, and recession of hazardous

materials [3]. Biomolecules such as proteins and nucleic acid [4], microbes [5], and plant extracts can be used to synthesize nanoparticles in both *in vivo* and *in vitro* studies [6, 7]. The complexation of phytochemicals or secondary metabolites with the nanoparticles is responsible for improved bioactivities and biocompatibilities [8, 9]. Leaf extracts act as both reducing and stabilizing agents in extremely efficient ways to synthesize metal and metal oxide NPs due to their ability to reduce metal ions faster than microbes, allowing for longer incubation times [10]. The primary process of green synthesis is the reduction of metal ions to crystallites, which are stabilized by reactive phytochemicals [11, 12].

Recently, metal oxides have drawn more interest because of their improved surface composition and larger surface area [13]. Metal oxide nanoparticles, including ZnO, MgO, CuO, CaO, Ag₂O, and TiO₂, are a new class of antimicrobial agents with potential applications in food, the environment, and healthcare

*Corresponding Author Dr. C. M. Kamanavalli, P. G. Department of Studies in Biochemistry, Karnatak University, Dharwad-580 003, India.
Tel: +91-9448922795; eMail: cmkamanavalli@gmail.com



DOI:10.62110/sciencein.mns.2025.v12.1184
URN:NBN:sciencein.mns.2025.v12.1184
© Authors, The ScienceIn
<https://pubs.thesciencein.org/jmns>



sectors [14]. These nanoscales (<100) inorganic materials have broad spectrum antibacterial activity, large surface area interaction, low resistance to bacteria, high stability, and tunable sizes, shapes, and chemical compositions [15]. The mechanism of metal oxide nanoparticle action on bacteria is complex and not fully understood. Numerous studies demonstrated that smaller particles have greater antibacterial activity due to higher reactive surface area [16]. Biogenic NPs are employed in medical treatments such as drug delivery, imaging, and as antimicrobial agents. Furthermore, biogenic NPs have demonstrated promising results in treating multidrug-resistant bacteria, making them a potential option in combating pathogenesis [17]. These green NPs can also be used in phytopathogen treatment in agriculture and water disinfection for environmental cleanup.

Magnesium oxides (MgO) are highly significant due to their distinct properties when compared to their bulk counterparts [18]. Magnesium oxide nanoparticles (MgO NPs) are exceptional due to their high electrical permittivity, chemical stability, strong photocatalytic activity, and lack of toxicity, making them potential long-lasting antimicrobial agents due to their low volatility and high-temperature tolerances [19]. MgO NPs are superior to conventional metal nanoparticles due to their distinctive physicochemical features, such as less toxicity, biocompatibility, stability, affordability, redox nature, cation capacity, biodegradability, and significant medicinal applications including analgesic, antibacterial, anticancer, anti-inflammatory, anti-diabetic, and bone-regenerating properties [20, 21].

Gmelina arborea, locally known as gamhar, it is a fast-growing deciduous tree belongs to the family *Lamiaceae*, and is an important plantation species in many tropical areas around the India. The species is naturally distributed in semi-deciduous forests in tropical/subtropical regions of South East Asia. The tree is also an important medicinal plant in the Indian systems of Medicine. The whole plant is used in medicine. The roots are acrid, bitter-sweet in taste, stomachic, tonic, laxative and antihelminthic. The flowers are sweet, refrigerant, bitter, astringent and acrid, and are used in treating leprosy and skin diseases. The fruits are acrid, sour, sweet, refrigerant, bitter, astringent, aphrodisiac, trichogenous, alterant and tonic. Fruits are edible and also used for promoting hair growth and in treating anaemia, leprosy, ulcers, constipation, leucorrhoea and colitis. The leaves are a good fodder also. Various studies demonstrated that *G. arborea* and its constituents possess several pharmacological activities like anti-oxidant, anti-diabetic, anti-inflammatory, antiulcer, analgesic, anti-nociceptive, anticancer and wound healing activities [22]. Our study explored novel approach to synthesizing MgO nanoparticles using *G. arborea* plant leaf extract as the reducing and capping agent. To evaluate the physicochemical characteristics of the MgO NPs, the different spectroscopic, morphological, and thermal tests were conducted. These tests included UV-vis, FTIR, XRD, DLS, SEM-EDX, HR-TEM, TGA, and DSC studies. The antimicrobial, antioxidant, and anti-angiogenic properties of the biosynthesized MgO NPs were further assessed.

MATERIALS AND METHODS

Chemical reagents

Magnesium chloride hexahydrate [MgCl₂.6H₂O] used in this experiment was of the highest purity and obtained from Sigma-Aldrich, St. Louis, MO (USA), sodium hydroxide (NaOH) from Hi-Media, Bangalore, India, nutrient agar, Muller-Hinton agar, 1,1-diphenyl-2-picrylhydroxyl (DPPH) from Sigma-Aldrich, St. Louis, MO (USA), ethanol, parafilm, from Hi-Media Bangalore, India. Milli-Q water was used in this experiment.

Collection of plant material

The fresh plant leaves were collected from the wild shrub territory in Western Ghat, Karnataka, India. The plant and its parts used in this study are freshly collected and identified as *G. arborea* by local botanist K. Kotresha, Karnatak University's College, Department of Botany, Dharwad, India.

Preparation of the *G. arborea* leaves extract

Fresh leaves were collected and washed with tap water and finally rinsed with Milli-Q (ultrapure type1 synergy UV), allowing them to be shade dried for 2 weeks. The dried leaves were crushed into fine powder and stored at room temperature for further use. The 10 g of fine powder of whole plant material of *G. arborea* boiled with 100 mL of double distilled water at 80 °C for 20 min, then cooled and filtered through muslin cloth followed by Whatman filter paper No 1. To make it clear solution mixture was centrifuged at 5000 rpm for 20 min the supernatant was stored at 4 °C for further use.

Synthesis of MgO nanoparticles

The MgO nanoparticles were prepared using *G. arborea* plant leaf extracts under mild conditions, with slight modifications of previously done by Nguyen et al (2021) [19]. Aqueous extract of *G. arborea* and MgCl₂.6H₂O (0.1M) solution were taken in the ratio 9:1 (v/v), subjected to continuous stirring for 4 h at 80 °C, add 20 mL NaOH (0.1M) dropwise to the solution mixture then the solution was kept overnight in the room temperature. The color develops from pale yellow to brown indicating the formation of magnesium oxide nanoparticles (MgO NPs). The reaction mixture was centrifuged at 8000 rpm for 20 min obtained pellets washed with water and further, the calcination was conducted at 450 °C for 4 h. The obtained powder was kept in a desiccator for further use.

Characterization of green synthesized MgO nanoparticles

The formation of MgO nanoparticles is observed by using UV-visible spectroscopy (UV Jasco Japan Make Model V670) ranges between 200-800 nm. The bioactive components containing functional groups found in the aqueous extract that are necessary for the synthesis of MgO NPs were evaluated by using a FTIR [Nicolet Thermo spectrophotometer iz10 instrument] in the wave number range of 4000 to 400 cm⁻¹. Dynamic light scattering (DLS) is used for measuring average particle diameter distribution of nano-sized particles dispersed in liquid using the analyzer [HORIBA, Nano particle analyzer SZ-100]. Zeta potential (ZP) is an analytical technique that evaluates the surface charge of NPs in colloidal solution. The magnitude of ZP predicts the colloidal stability. Lower dispersion ZP values will result in aggregation, coagulation, or flocculation because of van der waals interparticle interaction [6]. The stability of synthesized

MgO NPs were assessed by zeta potential (ZP). XRD analysis was used to characterize crystalline or semicrystalline materials, with Bragg's law as the primary regulation. (Make Rigaku Japan Model Smart labs). Scanning speed of the sample 10 °C/min at angle 2 θ . The surface morphological characteristics such as size, and shape of MgO NPs are examined by scanning electron microscopy-energy-dispersive X-ray spectroscopy (SEM-EDX) spectra were recorded on the S4800 high resolution scanning electron microscope [JEOL JSM-IT500 LA]. The differential scanning calorimetry (DSC) instrument (DSC Q20 V24.10 Build 122) was employed to assess the exothermic or endothermic reaction of NPs. Usually, the temperature ranges between 0 and 400 °C. Thermogravimetric analysis (TGA) was used to understand the thermal behaviours of materials that exhibit mass gain or loss due to oxidation, breakdown, or volatile loss (e.g., moisture and volatile organic compounds). (TA instrument SDT Q600) at a heating rate 10 °C/min. under nitrogen atmosphere [23-27].

Antibacterial activity

Green synthesized MgO NPs were analyzed for their antibacterial activity against human bacterial pathogens, including *B. subtilis*, *B. cereus*, *E. coli*, and *P. aeruginosa*. The evaluation was conducted using the well diffusion method [28] with slight modifications. Bacterial strains were subculture in nutrient broth at 37 °C until the suspension reached 1.5x10⁸ CFU/mL. Petri plates were then inoculated with different concentrations of MgO NPs, such as 25, 50, 75, and 100 μ g/mL, suspended in deionized water. The plates were incubated for 24 h at 37 °C, and the zone of inhibition was measured in triplicates.

Antioxidant activity

The green synthesized MgO NPs from *G. arborea* leaf extract was tested for their *in vitro* antioxidant activity using the 1' 1-diphenyl-2-picryl hydroxyl (DPPH) free radical scavenging assay [29]. The test involved adding varied concentrations MgO NPs to 3 mL of 0.1 mM DPPH solution and incubating for 30 min in the dark. The absorbance of the reaction mixture was measured at 517 nm using a UV-vis spectrophotometer, with ascorbic acid as the standard. The percentage of scavenging activity was calculated using equation (1).

DPPH radical scavenging (%) =

$$\frac{\text{Absorbance of control} - \text{Absorbance of sample}}{\text{Absorbance of control}} \times 100 \quad (1)$$

Anti-angiogenic properties

The chorioallantoic membrane (CAM) assay was performed with MgO NPs to test their antiangiogenic properties in chick embryos [30]. Fertilized eggs were obtained from a licensed poultry farm and sanitized with 70% ethanol. The eggs were placed in a CO₂ incubator at 37°C and 60% humidity. After 3 days of incubation, 2-4 mL of albumen was extracted from the egg, where a small hole was created at the pointed end. The eggs were then returned to the incubator. On the 5th day, a 1x1 cm window was made and treated with MgO NPs at varying concentrations (10, 20, and 40 μ g), while the control was treated with PBS. The eggs were sealed with parafilm and incubated for

3 days. The CAM assay imaged on the 8th day to show the effect of MgO NPs on capillary and microvessel networks. The experiment was performed in triplicate.

Statistical analysis

The experimental setups performed in triplicate, were analyzed using GraphPad Prism 8.0, with results presented as mean \pm SD. Comparisons were made using one-way ANOVA with a significance level of $p < 0.05$.

RESULTS AND DISCUSSION

UV-visible spectral studies

Phytoconstituents in plant extracts act as capping and reducing agents for nanoparticle synthesis, regulating particle size distribution and preventing clumping. The formation of MgO NPs was identified through color change, from pale yellow to dark brown precipitation due to reduction magnesium ions into MgO NPs. UV-visible spectral studies confirm the synthesis of MgO NPs within the wavelength range 200-800 nm. Figure 1 depicts absorption λ_{max} at 298 nm, indicating successful formation of MgO NPs. These results coincide with previously reported literature were Mg (OH)₂ NPs synthesized using the aqueous leaf extract of *Tinospora cordifolia* absorption peak at λ_{max} 289 nm [31]. The MgO absorption pattern around 300 nm reveals broad band gaps [32].

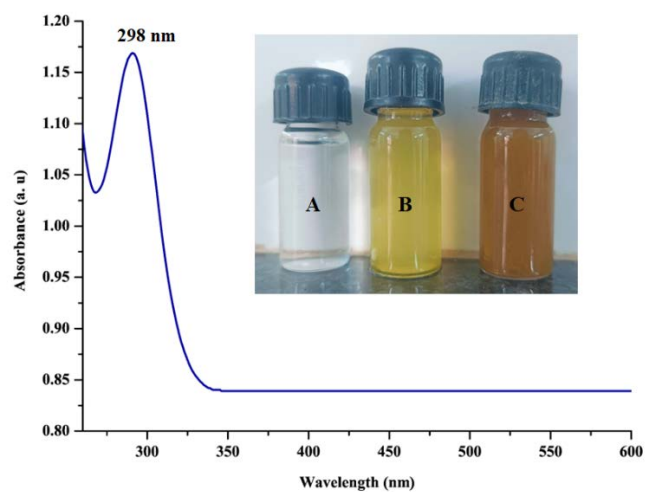


Figure 1. UV-visible absorption spectrum of MgO NPs (A-Precursor, B-Leaf extract and C-MgO NPs).

FTIR spectrum analysis

Fourier transform infrared spectroscopy (FTIR) analysis was performed to identify the functional groups present on both plant and on the surface of MgO NPs, which acts as the reducing and capping agents (Figure 2). The functional groups present in the leaf extract and MgO NPs are shown in Table 1. The absorption peak at 585 cm^{-1} , corresponds to the formation of MgO NPs from the *G. arborea* plant because of the metal-oxygen bond observed at 700-500 cm^{-1} [33, 34].

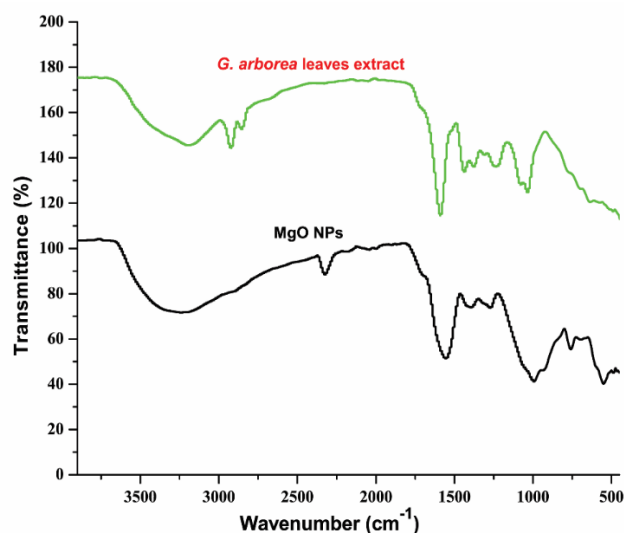


Figure 2. FTIR spectrum of leaf extract and MgO NPs.

Functional group	Wavenumber range (cm ⁻¹)	Leaf extract peak (cm ⁻¹)	MgO NPs peak (cm ⁻¹)	Peak details
O–H stretching	2500–3300	3191.67	3258.66	Strong and broad
O=C=O stretching	2200–2500	–	2358.48	Strong
C–H stretching	2840–3000	2851.70	–	Medium
N–H bending	1580–1650	1589.83	1582.45	Strong
O–H bending	1395–1440	1440.79	1420.13	Medium
C–O stretching	1220–1300	1224.82	1300.11	Strong
C–N stretching	1020–1250	1032.42	1023.47	Medium
C–H bending	790–840	–	790.77	medium
C–Cl stretching	550–850	–	585.64	Strong

Particle size and zeta potential of MgO NPs

The size distribution profiles of MgO NPs with a sub-micron level range can be measured *via* dynamic light scattering (DLS) analysis. The average particle size and zeta potential of MgO NPs produced by the *G. arborea* leaf extract. Figure 3 and 4 illustrate the average size of synthesized MgO NPs is 67±10 nm and Zeta potential of the synthesized MgO NPs is -36±5 mV respectively, these results lies between ±30 mV indicating the stability of the NPs [35]. The obtained NPs exhibit good stability for longer duration and smaller size of the NPs signifies its importance in

the field of biological applications (drug delivery, membrane permeable passage). These results were well matched with previous reported literature [36].

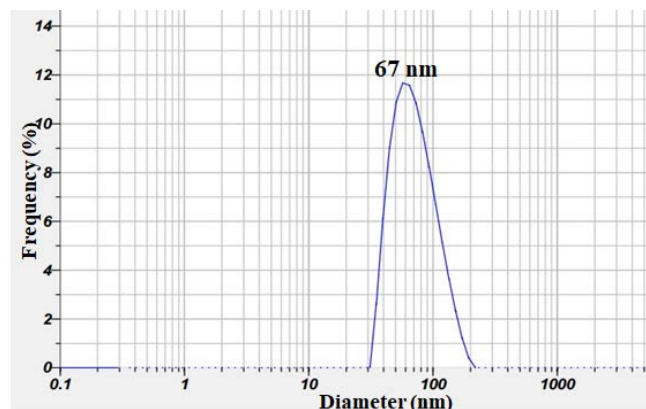


Figure 3. Particle size of MgO NPs.

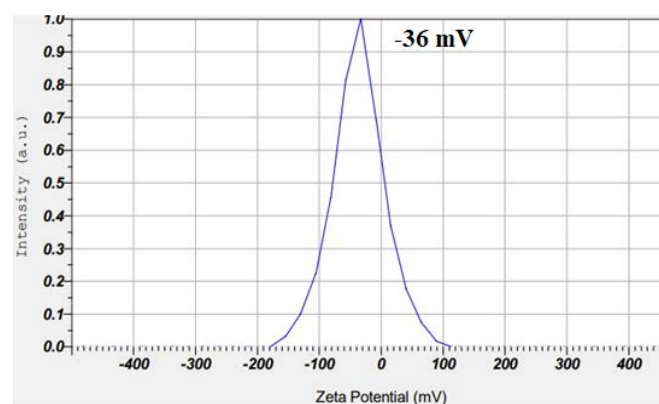


Figure 4. Zeta potential of the MgO NPs.

XRD analysis

The crystallographic nature of MgO NPs were identified by the X-ray diffraction patterns analysis with a 2θ values were found to be 27.44°, 31.74°, 45.54°, 56.39° and 75.28° they

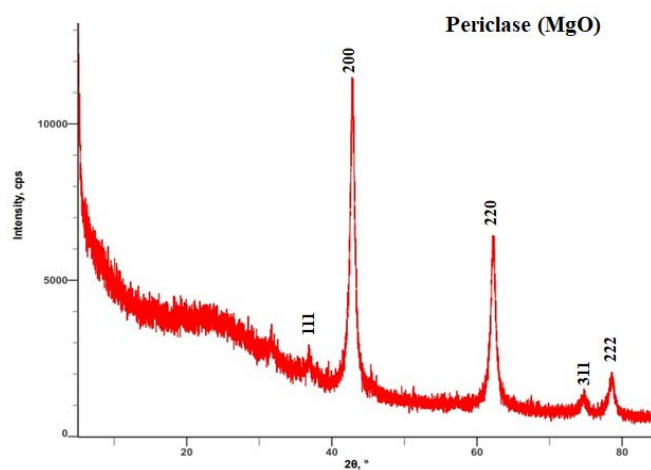


Figure 5. X-ray diffraction pattern of MgO NPs.

corresponds to the crystal planes (111), (200), (220), (222) and (311) respectively with reference no. (ICDD 01-080-4190, 4192). Figure 5 depicts the pure form periclase of MgO NPs and the average crystallite size was determined using the Debye-Scherrer equation (2), $d = k\lambda / (\beta \cos \theta)$ which was found to be 62 nm. The diffraction patterns of MgO NPs are well-compliant with the patterns of previous studies of Vijayakumar et al., (2021) [37].

Morphological analysis of MgO NPs

Scanning electron microscope was used to identify the size, distribution, and morphology of synthesized MgO NPs. The particles were roughly spherical shaped with unevenly distribution, and formed larger clusters, as seen in Figure 6a. Particle agglomeration may be due to the interactions and Van der waal's forces between MgO NPs [38]. The average size of the particles was found to be 30-50 nm. NPs of different sizes have useful applications in the field of medicine [39]. The elements present in the MgO NPs were identified using energy-dispersive X-ray spectroscopy (EDS). The EDX graph showed that the synthesized NPs were composed high amount of magnesium (Mg) and oxygen (O), less amount of carbon (C) silicon (Si) and chlorine (Cl) as shown in Figure 6b. Whereas the small peaks indicate that the synthesized MgO NPs show a negligible amount of other elemental impurities [40].

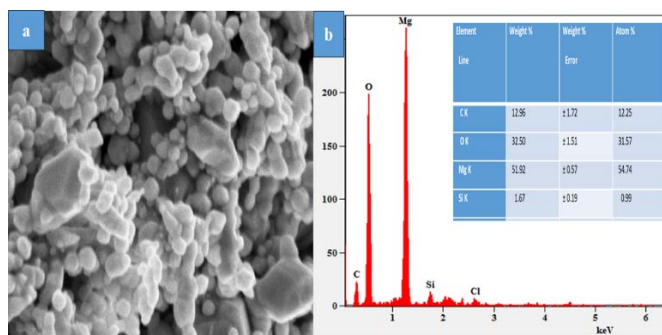


Figure 6. a) SEM images of MgO NPs. b) EDX spectrum of MgO NPs.

The TEM is used to measure the morphology of the NPs (Figure 7a and b). The TEM images showed that the central size of the MgO NPs, while dark spots in the organic matrix represent the phytochemicals enclosed by the extracts NPs [40]. A single particle with sphere-like shapes and rings can be found throughout the entire selected area electron diffraction (SAED) pattern. SAED pattern analysis confirms the single crystalline nature of MgO NPs, showing a spot pattern or bright dotted ring pattern (Figure 7b). The rings can be attributed to the crystal planes of MgO NPs corresponds to XRD results. The size distribution of the MgO NPs sample, assessed using Image J software, shows an average particle size between 30 and 60 nm (Figure 7d). A previous study found that the DLS measurement of MgO NPs particle size was significantly larger than the TEM measurement, due to differences in sample volume, particle counts, or optical properties [41].

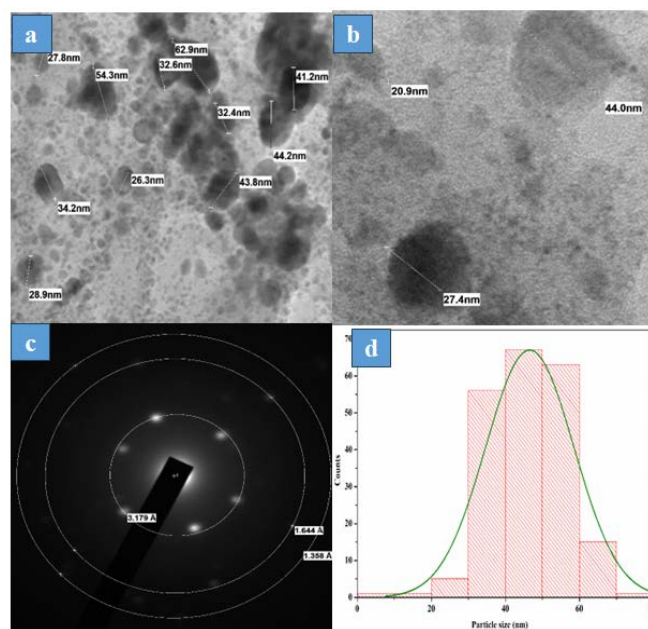


Figure 7. a) TEM images of MgO NPs. b) Single magnification of MgO NPs. c) SAED pattern of MgO NPs. d) particle size distribution of NPs.

TGA and DSC analysis

Studies on the thermal characteristics of the biologically produced MgO NPs were conducted using thermogravimetric analysis (TGA) and a differential scanning calorimeter (DSC). The TGA curve demonstrates multistage weight loss, i.e., 4.877% at 81.59 °C to 153.53 °C due to very low melting point components and the major weight loss at 271.23 °C to 315.25 °C, around 6.915%, which is due to absorption of moisture present on the MgO NPs. Around 502.33 °C to 529.03 °C and 661.89 °C to 702.40 °C little weight loss of 0.703 and 1.70% respectively, possibly due to the remaining lattice hydroxyls [42].

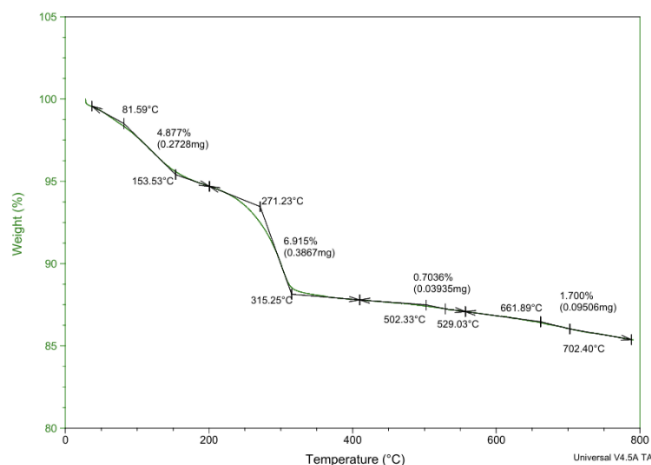


Figure 8. TG analysis of MgO NPs.

Differential scanning calorimetry (DSC) of MgO NPs plays an important role in exothermic processes. The DSC curve shows some peaks at 40.40 °C to 49.80 °C, 86 °C to 95.73 °C, 130 to

200 °C, and 228.09 to 238.90 °C with heat flows of 73.26, 645, 45.20, and 10.97 J/g respectively. These peaks represent exothermic events, which can indicate thermal transitions, phase transitions or reactions occurring in the MgO NPs as seen in Figure 9. A strong exothermic peak at 95.73 °C was observed, which implies the phase transition of Mg(OH)₂ to MgO formation. Hence, the pure MgO NPs were obtained at 500 °C and the obtained results are well consistent with previous reports [43].

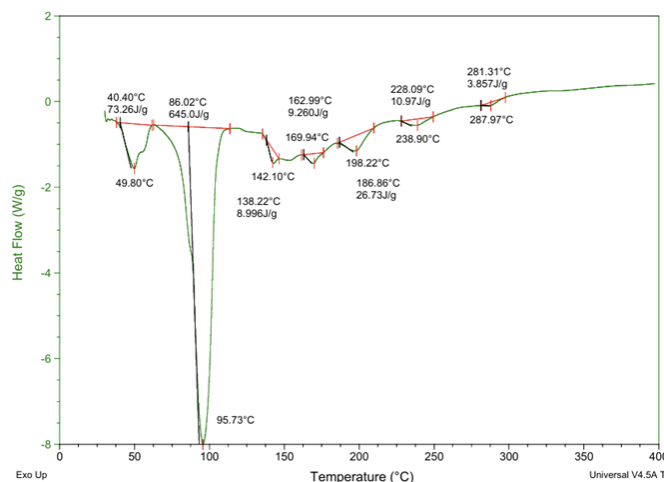


Figure 9. DSC analysis of MgO NPs.

Antibacterial study

The antibacterial activity of green synthesized MgO nanoparticles against Gram-positive and Gram-negative bacterial strains was examined using the well diffusion method for different concentrations (25, 50, 75 and 100 µg/mL). The results showed significant zone of inhibition for both strains (Figure 10) in dose dependent manner, which can be attributed to electrostatic interactions between opposing charges on bacterial cell walls and magnesium ions [33]. These results coincide with the previously reported literature of Hirphaye et al., (2023) where MgO NPs were synthesised using *Hagenia abyssinica* flower

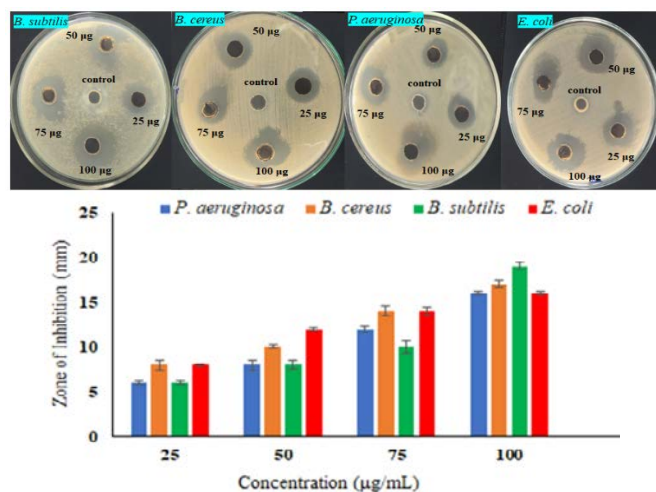


Figure 10. Zone of inhibition MgO NPs.

aqueous extract showed slightly greater activity for Gram-positive bacteria than the Gram-negative bacteria [44]. Hence, MgO NPs have potential antibacterial activity against human pathogens such as *B. cereus*, *B. subtilis*, *E. coli* and *P. aeruginosa* respectively.

Contact killing mechanism

The mechanism of metal oxide nanoparticle action on bacteria is complex and not fully understood. The impact of MgO nanoparticles on bacterial cell walls was investigated using *E. coli* (Figure 11). SEM images showed that the treated sample displayed an uneven and damaged cell wall, suggesting that MgO nanoparticles disrupt the cell wall, leading to bacterial cell death. This mechanism could be influenced by the difference in size of the nanoparticle. Gram-negative, due to the easier interaction with these Gram-positive bacteria causes disruption of the membrane structure of the bacteria's cell wall. Furthermore, Gram-positive bacteria have no outer membrane in their cell walls and a thick cell wall made up of multilayers of peptidoglycan. Gram-negative bacteria, on the other hand, have a more complicated cell wall structure, with a peptidoglycan layer between the outer and cytoplasmic membranes. Thus, Gram-positive bacteria's cell membranes are more easily destroyed [45]. A similar study investigated the effects of copper oxide nanoparticles (CuO NPs) on two bacterial strains, *E. coli* and *P. aeruginosa*, and found damage to cell membranes caused by CuO NPs. This aligns with previous literature, where green synthesized CuO nanoparticles, specifically Cu₂O, exhibit strong antibacterial properties [35].

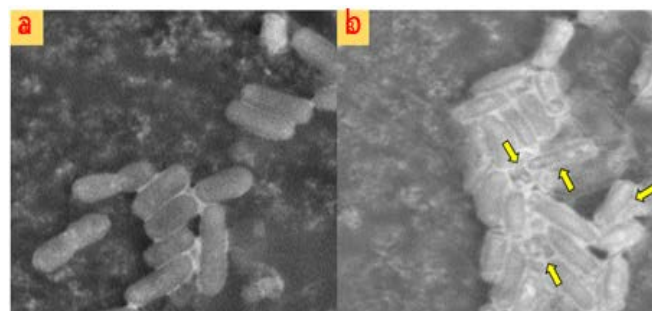


Figure 11. Contact killing mechanism a) Control b) MgO NPs treated bacteria.

MgO and CuO nanoparticles have higher antibacterial activities on Gram-positive bacteria than Gram-negative bacteria due to differences in cell membrane structure. Another study ZnO nanoparticles have shown strong activity against *C. jejuni* compared to *E. coli* O157:H7 or *Salmonella*, likely due to different tolerances to oxidative stress induced by nanoparticles [16].

Antioxidant activity

Antioxidants play a crucial role in regulating the metabolic processes of organisms, as they help prevent the generation of harmful free radicals and reactive oxygen species (ROS), which can lead to oxidative stress, tissue damage, and cell death [46]. The study found that plant extract and MgO NPs show antioxidant activity against DPPH in dose-dependently (20-640

$\mu\text{g/mL}$). The green synthesized MgO NPs shows greater DPPH scavenging activity than plant leaves extract (Figure 12) but slightly less than standard. The IC_{50} values of the green synthesized MgO NPs and leaf extract were 96.8 and 226.87 $\mu\text{g/mL}$, respectively. These results are well corresponded with that of previous reports by Ammulu et al. (2021), which found the green synthesized MgO NPs IC_{50} value 72.24 $\mu\text{g/mL}$ to possess significant antioxidant properties [40]. Similarly, Dobrucia reported antioxidant activity of MgO NPs synthesised using *Artemisia abrotanum* herba extract [47].

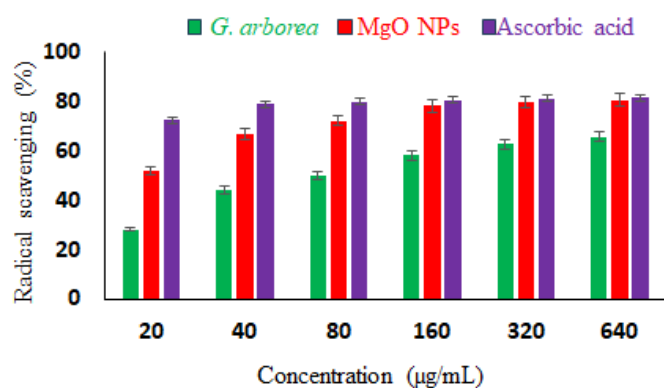


Figure 12. Antioxidant activity of *G. arborea*, MgO NPs and Ascorbic acid.

Ant-angiogenic activity

The study examined the anti-angiogenic effect of MgO NPs on chick embryos in dose dependent manner. Results showed that MgO NPs treated chick embryo showed inhibition for new blood vessel development compared to control (Figure 13). As lower dose of MgO NPs treated embryos inhibited the formation of new capillaries and branching without affecting mature blood vessels. MgO nanoparticles demonstrated a significant reduction in blood vessel count and complete disruption of embryos at higher doses (40 μg). MgO NPs had potential anti-angiogenic properties. The mechanism of angiogenesis is the process of vascularizing new blood vessels during the metastatic stage of a tumor, which can be prevented to reduce onco-cell colonization in other parts of the body, as cancer cells are carried by these vessels [35].



Figure 13. Anti-angiogenic activity of MgO NPs.

CONCLUSION

The study highlights the pioneer approach for synthesizing MgO NPs using a wild wood species *G. arborea* leaf extract as a natural source. This green technology paved the way for an economically and eco-friendly approach. According to FTIR

spectrum analysis of the *G. arborea* extract contains few phytochemicals that facilitate the reduction and stabilizing MgO NPs. The average crystallite size of the synthesized NPs was found to be 42 nm. DLS results shows the size and stability of MgO NPs which helps in biomedical applications. MgO NPs showed antimicrobial properties for both Gram-positive and Gram-negative bacterial strains. The antioxidant properties of MgO nanoparticles, with an average IC_{50} value of 96.8 $\mu\text{g/mL}$, confirm their potential in neutralizing DPPH free radicals. MgO NPs exhibit anti-angiogenic properties, which inhibit new blood vessel formation essential for tumor growth. The study suggests MgO NPs as a potential biomaterial for biological, pharmacological, eco-friendly, and safe processes.

CREDIT AUTHORS CONTRIBUTION

Parashuram Shivappa: Conceptualization, Data interpretation, Investigation, Methodology, Validation, Visualization, Writing-original draft; Anjana Thatesh Gaddigal: Methodology, Writing-review & editing; Paramanna Bhagappa Poojari: Writing-review & editing; Kirankumar Malleshappa Irannanavar: Writing-review & editing; Praveen Veerappa Huyilgola: Writing-review & editing; Shanmukappa Veerabadrappa Irannanavar: Writing-review & editing; Chandrappa Mukappa Kamanavalli: Project administration, Writing-review & editing.

ACKNOWLEDGEMENT

The authors would like to express our thanks to the University Scientific and Instrumentation Center (USIC), Karnatak University, Dharwad, India, for providing the instrumentation facilities utilized in characterizations. The authors would like to thank Sophisticated Analytical Instrument Facilities (SAIF) Kolhapur, India for providing TEM instrumentation facility.

DECLARATION OF INTEREST

The authors declare that they have no known competing financial interests or personal relationships that could have appeared to influence the work reported in this paper.

REFERENCES AND NOTES

- G. Sharma, R. Soni, N.D. Jasuja. Phytoassisted synthesis of magnesium oxide nanoparticles with *Swertia chirayaita*. *J. Taibah Univ. Sci.* **2017**, 11 (3), 471–477.
- N. Joudeh, D. Linke. Nanoparticle classification, physicochemical properties, characterization, and applications: a comprehensive review for biologists. *J. Nanobiotechnol.* **2022**, 20 (1), 262.
- F. Khan, M. Shariq, M. Asif, et al. Green Nanotechnology: Plant-Mediated Nanoparticle Synthesis and Application. *Nanomaterials* **2022**, 12 (4), 673.
- Y. Leng, L. Fu, L. Ye, et al. Protein-directed synthesis of highly monodispersed, spherical gold nanoparticles and their applications in multidimensional sensing. *Sci. Rep.* **2016**, 6 (1), 28900.
- H. Barabadi, B. Tajani, M. Moradi, et al. Penicillium Family as Emerging Nanofactory for Biosynthesis of Green Nanomaterials: A Journey into the World of Microorganisms. *J. Clust. Sci.* **2019**, 30 (4), 843–856.
- F.B. Moreno-Luna, A. Tovar-Corona, J.L. Herrera-Perez, et al. Quick synthesis of gold nanoparticles at low temperature, by using *Agave potatorum* extracts. *Mater. Lett.* **2019**, 235, 254–257.
- D. Garibo, H.A. Borbón-Núñez, J.N.D. de León, et al. Green synthesis of silver nanoparticles using *Lysiloma acapulcensis* exhibit high-antimicrobial activity. *Sci. Rep.* **2020**, 10 (1), 12805.

8. S. Sudhasree, A. Shakila Banu, P. Brindha, G.A. Kurian. Synthesis of nickel nanoparticles by chemical and green route and their comparison in respect to biological effect and toxicity. *Toxicol. Environ. Chem.* **2014**, 96 (5), 743–754.
9. R. Augustine, A. Hasan. Emerging applications of biocompatible phytosynthesized metal/metal oxide nanoparticles in healthcare. *J. Drug Deliv. Sci. Technol.* **2020**, 56, 101516.
10. J.R. Shaikh, M. Patil. Qualitative tests for preliminary phytochemical screening: An overview. *Int. J. Chem. Stud.* **2020**, 8 (2), 603–608.
11. J. Singh, T. Dutta, K.H. Kim, et al. “Green” synthesis of metals and their oxide nanoparticles: Applications for environmental remediation. *J. Nanobiotechnol.* **2018**, 16 (1), 84.
12. H. Chandra, P. Kumari, E. Bontempi, S. Yadav. Medicinal plants: Treasure trove for green synthesis of metallic nanoparticles and their biomedical applications. *Biocatal. Agric. Biotechnol.* **2020**, 24, 101518.
13. A.A. Hussain, S. Nazir, R. Irshad, et al. Synthesis of functionalized mesoporous Ni-SBA-16 decorated with MgO nanoparticles for Cr (VI) adsorption and an effective catalyst for hydrodechlorination of chlorobenzene. *Mater. Res. Bull.* **2021**, 133, 111059.
14. D.C. Luther, R. Huang, T. Jeon, et al. Delivery of drugs, proteins, and nucleic acids using inorganic nanoparticles. *Adv. Drug Deliv. Rev.* **2020**, 156, 188–213.
15. X. Li, S.M. Robinson, A. Gupta, et al. Functional gold nanoparticles as potent antimicrobial agents against multi-drug-resistant bacteria. *ACS Nano* **2014**, 8 (10), 10682–10686.
16. Y. Xie, Y. He, P.L. Irwin, T. Jin, X. Shi. Antibacterial activity and mechanism of action of zinc oxide nanoparticles against *Campylobacter jejuni*. *Appl. Environ. Microbiol.* **2011**, 77 (7), 2325–2331.
17. D.C. Luther, R. Huang, T. Jeon, et al. Delivery of drugs, proteins, and nucleic acids using inorganic nanoparticles. *Adv. Drug Deliv. Rev.* **2020**, 156, 188–213.
18. S. Kaur, J. Singh, R. Rawat, et al. A smart LPG sensor based on chemo-bio synthesized MgO nanostructure. *J. Mater. Sci. Mater. Electron.* **2018**, 29 (14), 11679–11687.
19. D.T.C. Nguyen, H.H. Dang, D.V.N. Vo, et al. Biogenic synthesis of MgO nanoparticles from different extracts (flower, bark, leaf) of *Tecoma stans* (L.) and their utilization in selected organic dyes treatment. *J. Hazard. Mater.* **2021**, 404, 124146.
20. Y.H. Leung, A.M.C. Ng, X. Xu, et al. Mechanisms of antibacterial activity of mgo: Non-ros mediated toxicity of mgo nanoparticles towards *escherichia coli*. *Small* **2014**, 10 (6), 1171–1183.
21. Y. He, S. Ingudam, S. Reed, et al. Study on the mechanism of antibacterial action of magnesium oxide nanoparticles against foodborne pathogens. *J. Nanobiotechnol.* **2016**, 14 (1), 54.
22. R.R. Warriar, S.M. Priya, R. Kalaiselvi. Gmelina arborea– an indigenous timber species of India with high medicinal value: A review on its pharmacology, pharmacognosy and phytochemistry. *J. Ethnopharmacol.* **2021**, 267, 113593.
23. J. Dolai, K. Mandal, N.R. Jana. Nanoparticle Size Effects in Biomedical Applications. *ACS Appl. Nano Mater.* **2021**, 4 (7), 6471–6496.
24. S. Mourdikoudis, R.M. Pallares, N.T.K. Thanh. Characterization techniques for nanoparticles: Comparison and complementarity upon studying nanoparticle properties. *Nanoscale* **2018**, 10 (27), 12871–12934.
25. V. Holišová, M. Urban, Z. Konvičková, et al. Colloidal stability of phytosynthesized gold nanoparticles and their catalytic effects for nerve agent degradation. *Sci. Rep.* **2021**, 11 (1), 4071.
26. E. Ghanbari, S.J. Picken, J.H. van Esch. Analysis of differential scanning calorimetry (DSC): determining the transition temperatures, and enthalpy and heat capacity changes in multicomponent systems by analytical model fitting. *J. Therm. Anal. Calorim.* **2023**, 148 (22), 12393–12409.
27. A.T. Odularu. Metal Nanoparticles: Thermal Decomposition, Biomedical Applications to Cancer Treatment, and Future Perspectives. *Bioinorg. Chem. Appl.* **2018**, 2018, 9354708.
28. N.Y.T. Nguyen, N. Grelling, C.L. Wetteland, R. Rosario, H. Liu. Antimicrobial Activities and Mechanisms of Magnesium Oxide Nanoparticles (nMgO) against Pathogenic Bacteria, Yeasts, and Biofilms. *Sci. Rep.* **2018**, 8 (1), 16260.
29. M.P. Ganeshkar, A.T. Gaddigal, P. Shivappa, et al. Biocompatibility assessment of Rutin and PEG loaded novel nanoceria on human erythrocytes and human myeloid leukemia (U937) cells. *J. Drug Deliv. Sci. Technol.* **2023**, 86, 104761.
30. P. Shivappa, M.R. Mirjankar, A.T. Gaddigal, et al. Bismuth nanoparticle synthesis utilizing hydroalcoholic *Endocoma macrocoma* leaf extract to evaluate their antimicrobial, antioxidant, and anticancer properties. *J. Dispers. Sci. Technol.* **2025**, 2025, 1–15.
31. M. Rajkumar, S.I.D. Presley, F. Menaa, et al. Biosynthesis and biological activities of magnesium hydroxide nanoparticles using *Tinospora cordifolia* leaf extract. *Bioprocess Biosyst. Eng.* **2024**, 47 (12), 2111–2129.
32. R.H. Alrashoudi, M. Abudawood, A. Mateen, et al. Characterization and antimicrobial, antioxidant, and anti-proliferative activities of green synthesized magnesium oxide nanoparticles with shoot extracts of *Platocarpus curviflorus*. *Asian Pac. J. Trop. Biomed.* **2023**, 13 (7), 315–324.
33. R.B. Rotti, D. V. Sunitha, R. Manjunath, et al. Green synthesis of MgO nanoparticles and its antibacterial properties. *Front. Chem.* **2023**, 11, 1143614.
34. A. Ananda, T. Ramakrishnappa, S. Archana, et al. Green synthesis of MgO nanoparticles using *Phyllanthus emblica* for Evans blue degradation and antibacterial activity. *Mater. Today Proc.* **2021**, 49, 801–810.
35. A.T. Gaddigal, P. Shivappa, M.P. Ganeshkar, et al. Green synthesis of copper oxide nanoparticles using *Simarouba glauca* leaf extract, characterization and screening for their biological applications. *J. Dispers. Sci. Technol.* **2024**, 2024, 1–15.
36. A. Pugazhendhi, R. Prabhu, K. Muruganatham, R. Shanmuganathan, S. Natarajan. Anticancer, antimicrobial and photocatalytic activities of green synthesized magnesium oxide nanoparticles (MgONPs) using aqueous extract of *Sargassum wightii*. *J. Photochem. Photobiol. B Biol.* **2019**, 190, 86–97.
37. S. Vijayakumar, M. Nilavukkarasi, P.K. Praseetha. Synthesis of MgO nanoparticles through green method and evaluation of its antimicrobial activities. *Vegetos* **2021**, 34 (3), 719–724.
38. E.R. Essien, V.N. Atasie, A.O. Okeafor, D.O. Nwude. Biogenic synthesis of magnesium oxide nanoparticles using *Manihot esculenta* (Crantz) leaf extract. *Int. Nano Lett.* **2020**, 10 (1), 43–48.
39. S. Narendhran, M. Manikandan, P. Baby Shakila. Antibacterial, antioxidant properties of *Solanum trilobatum* and sodium hydroxide-mediated magnesium oxide nanoparticles: A green chemistry approach. *Bull. Mater. Sci.* **2019**, 42 (3), 133.
40. M.A. Ammulu, K. Vinay Viswanath, A.K. Giduturi, et al. Phytoassisted synthesis of magnesium oxide nanoparticles from *Pterocarpus marsupium* rox.b heartwood extract and its biomedical applications. *J. Genet. Eng. Biotechnol.* **2021**, 19 (1), 21.
41. J. Jeevanandam, Y.S. Chan, M.K. Danquah. Biosynthesis and characterization of MgO nanoparticles from plant extracts via induced molecular nucleation. *New J. Chem.* **2017**, 41 (7), 2800–2814.
42. A.F. Farizan, H.M. Yusoff, N. Badar, et al. Green Synthesis of Magnesium Oxide Nanoparticles Using *Mariposa christia vespertilionis* Leaves Extract and Its Antimicrobial Study Toward *S. aureus* and *E. coli*. *Arab. J. Sci. Eng.* **2023**, 48 (6), 7373–7386.
43. A. Venkatachalam, J.P. Jesuraj, K. Sivaperuman. *Moringa oleifera* Leaf Extract-Mediated Green Synthesis of Nanostructured Alkaline Earth Oxide (MgO) and Its Physicochemical Properties. *J. Chem.* **2021**, 2021, 1–22.
44. B.Y. Hirphaye, N.B. Bonka, A.M. Tura, G.M. Fanta. Biosynthesis of magnesium oxide nanoparticles using *Hagenia abyssinica* female flower aqueous extract for characterization and antibacterial activity. *Appl. Water Sci.* **2023**, 13 (9), 175.
45. J. Maji, S. Pandey, S. Basu. Synthesis and evaluation of antibacterial properties of magnesium oxide nanoparticles. *Bull. Mater. Sci.* **2020**, 43 (1), 25.
46. R. Periakaruppan, B. Ariuthayan, P. Vanathi, et al. Fabrication of Allium cepa-assisted magnesium oxide nanoparticles with antibacterial and antioxidant properties. *Biomass Convers. Biorefinery* **2023**, 1–8.
47. R. Dobrucka. Synthesis of MgO Nanoparticles Using *Artemisia abrotanum* Herba Extract and Their Antioxidant and Photocatalytic Properties. *Iran. J. Sci. Technol. Trans. A Sci.* **2018**, 42 (2), 547–555.